

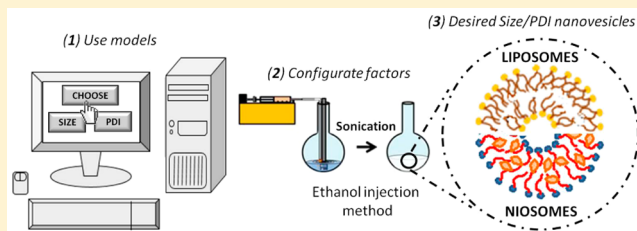
Using Factorial Experimental Design to Prepare Size-Tuned Nanovesicles

Pablo García-Manrique,^{†,‡} María Matos,[†] Gemma Gutiérrez,[†] Oscar R. Estupiñán,^{†,‡} María Carmen Blanco-Lopez,[‡] and Carmen Pazos^{*,†}

[†]Department of Chemical and Environmental Engineering and [‡]Department of Physical and Analytical Chemistry, University of Oviedo, Julián Clavería 8, 33006 Oviedo, Spain

Supporting Information

ABSTRACT: The aim of this work was to prepare size-tuned nanovesicles using a modified ethanol injection method (EIM) by applying factorial experimental design. Stable size-tuned nanovesicles (liposomes and niosomes) with controlled sizes and high EE values for hydrophobic compounds (Sudan Red 7B and vitamin D₃) were achieved. Equations that were able to predict the mean particle sizes, in the ranges of 55–156 nm for liposomes and 224–362 nm for niosomes with PDI values between 0.032 and 0.378, were obtained. These customized soft nanoparticles could be suitable in food, cosmetic, pharmaceutical, or medical applications, such as diagnosis or therapy.



1. INTRODUCTION

Controlled preparation of nanoparticles has attracted great interest in recent years.¹ Nanovesicles are an important family of organic nanoparticles, produced by bottom-up nanotechnology, with relevant applications in biomedicine,² food science,³ analytical chemistry,^{4,5} and biosensors.⁶ They are considered soft nanoparticles because interactions among their molecular components are similar to those arising from biological systems.⁷ Most of the work describing their preparation for specific uses has focused on the optimization of their composition with the aim of maximizing encapsulation efficiency, delivery, or delivery control.

However, size is one of the most critical properties (together with shape and surface chemistry) for understanding cell-uptake processes and, therefore, bioavailability and targetability.⁷ Several studies have focused on the optimization of the drug encapsulation efficiency while considering size as just a property for controlling administration parameters, such as penetration kinetics in topical formulations. For example, Padamwar et al.⁸ studied the encapsulation of vitamin E in liposomes and found that the amount of lipids yielded a positive correlation with size, which was, in turn, negatively correlated with penetration efficiency into the skin. Sometimes, size has been found to increase with higher amounts of membrane components, such as cholesterol, whereas it decreased with higher amounts of surfactants (e.g., Tween 80). Simultaneously, cholesterol or surfactants can affect encapsulation efficiency (EE). Optimal situations can be reached as a compromise at intermediate levels of both factors. In that case, Taha⁹ also reported an interaction between membrane-component concentration and size reduction by ultrasound, making factor optimization an essential task. In other cases, an opposite effect was observed, and higher concentrations of membrane components (such as Span 60 and

cholesterol) produced larger sizes and increased EEs. It is useful to deliver efficient amounts of a selected drug into superficial skin layers without systemic absorption.¹⁰ On this basis, the goal of our work was to set up a bulk method for producing nanovesicles of controlled size that could be subsequently modified for specific applications.

Vesicles are colloidal particles in which a concentric bilayer made up of amphiphilic molecules surrounds an aqueous compartment. These vesicles are commonly used to encapsulate both hydrophilic and lipophilic compounds, for food, cosmetic, pharmaceutical, or medical applications, such as diagnosis or therapy.¹¹ Hydrophilic compounds are entrapped into the aqueous compartments between bilayers, whereas lipophilic compounds are preferentially located inside the bilayers.^{12,13} The most common types of vesicles are liposomes and niosomes.

Liposomes were first described by Bangham et al. in 1965,¹⁴ and they are basically spherical bilayer vesicles formed by the self-assembly of phospholipids. This self-assembly process is based on the interactions occurring between phospholipids and water molecules, where the polar head groups of phospholipids are exposed to the aqueous phases (inner and outer) and the hydrophobic hydrocarbon tails are forced to face each other in a bilayer.¹⁵ Because of the presence of both lipid and aqueous phases in liposome structures, they can be used for the encapsulation, delivery, and controlled release of hydrophilic, lipophilic, and amphiphilic compounds.^{15,16}

On the other hand, niosomes are vesicles formed by the self-assembly of nonionic surfactants in aqueous media resulting in

Received: April 21, 2016

Revised: July 28, 2016

Accepted: August 10, 2016

Table 1. Plackett–Burman Fractional Factorial Design: Responses, Levels, and Factors

response code		meaning												
Y_1		Z-average size of PC liposomes												
Y_2		PDI of PC liposomes												
factors														
formulation				injection				evaporation			sonication			
level	O/A (X_1)	C (X_2) (g/L)	I (X_3) (mM)	Q_V (X_4) (mL/h)	T_1 (X_5) ($^{\circ}$ C)	N_S (X_6) (rpm)	T_E (X_7) ($^{\circ}$ C)	N_R (X_8) (rpm)	A (X_9) (%)	t (X_{10}) (min)				
–1	5:50	2.5	10	50	30	350	35	30	25	15				
1	20:50	6.0	150	215	60	900	60	120	42	30				
batch	X_1	X_2	X_3	X_4	X_5	X_6	X_7	X_8	X_9	X_{10}	Y_1	Y_2		
PB1	1	1	–1	–1	–1	–1	1	–1	1	1	90	0.254		
PB2	1	–1	–1	1	–1	1	1	1	1	–1	93	0.129		
PB3	–1	–1	–1	–1	–1	–1	1	1	–1	–1	97	0.152		
PB4	1	–1	1	–1	1	0	1	–1	1	–1	72	0.205		
PB5	–1	1	–1	1	–1	–1	1	–1	–1	1	258	0.413		
PB6	1	1	1	1	–1	–1	–1	1	–1	–1	102	0.176		
PB7	–1	–1	1	1	–1	–1	–1	–1	1	1	84	0.218		
PB8	1	–1	–1	1	1	1	–1	1	–1	1	106	0.240		
PB9	–1	–1	–1	–1	1	1	–1	1	1	1	71	0.229		
PB10	1	–1	1	–1	–1	–1	–1	–1	–1	1	81	0.141		
PB11	–1	1	1	–1	1	–1	1	1	–1	1	152	0.316		
PB12	1	1	1	1	1	1	1	1	1	1	65	0.260		
PB13	–1	–1	1	1	1	1	1	–1	–1	–1	87	0.189		
PB14	–1	1	1	–1	–1	1	–1	1	1	–1	115	0.273		
PB15	1	1	–1	–1	1	1	–1	–1	–1	–1	113	0.199		
PB16	–1	1	–1	1	1	–1	–1	–1	1	–1	74	0.271		

78 closed bilayer structures.^{13,17,18} As liposomes, their formation
 79 process is a consequence of unfavorable interactions between
 80 surfactants and water molecules, and they can also entrap
 81 hydrophilic, lipophilic, and amphiphilic compounds.^{19,20}

82 Niosomes exhibit a number of advantages over liposomes,
 83 such as higher stability, easy access to raw materials, lower
 84 toxicity, high compatibility with biological systems, non-
 85 immunogenicity, and versatility for surface modification.²⁰

86 Cholesterol is commonly used as a membrane additive for
 87 nanovesicle preparation to improve vesicle stability, entrapment
 88 efficiency, and release under storage.²⁰ It increases vesicle size
 89 and rigidity, improving encapsulation efficiency, but at high
 90 concentrations, it can adversely affect the encapsulation rate.^{21,22}

91 Cholesterol also plays a fundamental role in niosome formation
 92 when hydrophilic surfactants are used (hydrophile/lipophile
 93 balance of ~ 10).²⁰

94 More than 20 different methods have been identified for
 95 nanovesicle preparation, and these methods were recently
 96 reviewed.^{23,24} In this work, a modified ethanol injection method
 97 (EIM) is used, because it offers some advantages over other
 98 methods, such as simplicity, absence of potentially harmful
 99 chemicals, and suitability for scaleup.²⁵

100 The conventional EIM was first described in 1973.²⁶ In this
 101 technique, lipids/surfactants and additives are first dissolved in
 102 an organic solvent, such as diethyl ether or ethanol, and then
 103 injected slowly through a syringe into an aqueous phase
 104 containing the compound of interest. Then, the organic solvent
 105 is removed using a vacuum rotary evaporator. When ethanol is
 106 used as the organic solvent, the spontaneous formation of
 107 vesicles occurs as soon as the organic solution is in contact with
 108 the aqueous phase,²⁷ but vigorous agitation is needed to obtain
 109 narrow size distributions. For this purpose, a final sonication
 110 stage was applied in this study after organic-phase removal by
 111 vacuum evaporation.

112 However, a large number of variables are involved in this
 113 modified EIM, and selection of the most important of them
 114 (screening) is a crucial step in rationally preparing vesicles by this
 115 versatile method. In this work, the Z-average size and
 116 polydispersity index (PDI) were selected as the dependent
 117 variables. They are considered to be of great importance in
 118 nanovesicle design because most of the final applications of these
 119 vesicular systems are directly related to these two parameters.
 120 Factorial experimental design and the analysis of variance
 121 (ANOVA) methodology are appropriate and efficient statistical
 122 tools that permit the effects of several factors that influence
 123 responses to be studied by varying the factors simultaneously in a
 124 limited number of experiments.

125 In the recent past, design of experiments (DoE) has been
 126 extensively used for the study and optimization of vesicles and
 127 other similar organic materials. Different designs can be applied
 128 to reduce the number of factors involved in the preparation
 129 techniques²⁸ and, therefore, to minimize the number of
 130 experiments without losing valuable information. Plackett–
 131 Burman design is a type of fractional design involving relatively
 132 few runs,²⁹ commonly used for the screening of variables.

133 Another important role of DoE is in the optimization of
 134 nanovesicle composition for the enhancement of intended
 135 purposes. For instance, it has been applied to the formulation of
 136 liposomes (phospholipid and cholesterol ratio) for the topical
 137 delivery of vitamin E,⁸ hybrid liposomes (with both low- and
 138 high-transition-temperature phospholipids) to improve the
 139 encapsulation and delivery of silymarin,³⁰ and niosomes for
 140 topical delivery applications.^{10,31} DoE has also been used to
 141 enhance the transdermal flux of raloxifene hydrochloride³² and
 142 diclofenac diethylamine³³ loaded transfersomes and of other
 143 polymeric nanoparticles encapsulating an anticancer drug.³⁴
 144 Moreover, the interactions between vesicles and proteins, such as
 145 pectin, to improve drug-delivery properties has been studied by

146 DoE.³⁵ Nanostructured lipid carriers (NLCs) loaded with
147 flurbiprofen were also produced under optimal conditions
148 using full factorial design.³⁶

149 In this work, an initial fractional factorial design with two levels
150 (Plackett–Burman) was used to screen the most important
151 factors in vesicle preparation by the EIM. Then, a 2³ two-level full
152 factorial design using center-point replicates was applied to study
153 the influence of the main factors and their interactions on the Z-
154 average size and PDI. Once the appropriate operating conditions
155 were determined, vesicle stability was studied by using multiple
156 light scattering technology and by measuring the encapsulation
157 efficiencies (EEs) of different compounds.

2. MATERIALS AND METHODS

158 **2.1. Materials.** Phosphatidylcholine (PC) (predominant
159 species C₄₂H₈₀NO₈P, MW = 775.04 g/mol) from soybean
160 (Phospholipon 90G) was a kind gift from Lipoid (Ludwigshafen,
161 Germany). Sorbitan monostearate (Span 60, S60) (C₂₄H₄₆O₆,
162 MW = 430.62 g/mol) and cholesterol (Cho) (C₂₇H₄₆O, MW =
163 386.65 g/mol) were purchased from Sigma-Aldrich (St. Louis,
164 MO). All membrane components were dissolved in absolute
165 ethanol (Sigma-Aldrich, St. Louis, MO).

166 Methanol, acetonitrile, 2-propanol, and acetic acid of high-
167 performance liquid chromatography (HPLC) grade were
168 supplied by Sigma-Aldrich (St. Louis, MO).

169 A phosphate buffer (PB) solution (10 mM, pH 7.4) was used
170 in all experiments as the aqueous phase. The buffer solution was
171 prepared in Milli-Q water by dissolving proper amounts of
172 sodium dihydrogen phosphate and sodium hydrogen phosphate,
173 supplied by Panreac (Barcelona, Spain). Sodium chloride from
174 Panreac (Barcelona, Spain) was added to increase the ionic
175 strength when required according to the experiments listed in
176 Table 1. For the encapsulation experiments, Fat Red Bluish or
177 Sudan Red 7B dye (C₂₄H₂₁N₅, MW = 379.46 g/mol) and
178 cholecalciferol or vitamin D₃ (C₂₇H₄₄O, MW = 384.64 g/mol)
179 were purchased from Sigma-Aldrich (St. Louis, MO).

180 **2.2. Factorial Design of Experiments.** Factors that could
181 potentially affect the size of vesicles produced by the EIM were
182 classified in four groups, according to the different steps involved
183 in this preparation method: formulation (organic/aqueous phase
184 volume ratio, phospholipid concentration, and ionic strength),
185 injection (injection flow rate, temperature, and stirring speed),
186 evaporation (temperature and rotation speed), and sonication
187 (amplitude and time of sonication).

188 To identify the relative effects of variables on the response, a
189 two-level fractional factorial design was used. A Plackett–
190 Burman (P–B) resolution III design with $n = 16$ runs was
191 proposed for screening of the initial factors. Two levels were
192 selected for each variable.

193 Table 1 lists the factors and levels involved in the P–B
194 fractional factorial design used, where O/A is the organic/
195 aqueous phase volume ratio, C is the concentration of
196 phospholipid, I is the ionic strength, Q_V is the injection flow
197 rate, T_I is the injection temperature, N_S is the stirring speed
198 during injection, T_E is the evaporation temperature, N_E is the
199 evaporator rotation speed, A is the sonication amplitude, and t is
200 the sonication time.

201 In a second step, a 2³ full factorial design with center-point
202 repetitions ($n = 5$) was carried out to study the main effects and
203 interactions between factors previously selected by the screening
204 design (Table 2). All other factors were fixed at certain values.

205 In both designs, mean diameter (Z-average size) and PDI were
206 selected as response variables. Minitab statistical software

Table 2. Full Factorial Design (2³) with Center-Point Repetitions ($n = 5$): Factors, Levels, and Responses

response code		meaning	
Y ₁		Z-average size of PC liposomes	
Y ₂		PDI of PC liposomes	
Y ₃		Z-average size of S60:Cho niosomes	
Y ₄		PDI of S60:Cho niosomes	
factors			
level	O/A (X ₁)	C (X ₂) (g/L)	A (X ₃) (%)
−1 (low)	5:50	2	30
0 (medium)	12.5:50	5	42.5
1 (high)	20:50	8	55

batch	X ₁	X ₂	X ₃	Y ₁	Y ₂	Y ₃	Y ₄
FF1	1	−1	1	65	0.299	305	0.075
FF2	1	1	−1	97	0.249	362	0.136
FF3	−1	1	−1	149	0.296	294	0.206
FF4	−1	1	1	88	0.307	262	0.291
FF5	−1	−1	1	64	0.342	242	0.120
FF6	1	1	−1	100	0.257	360	0.143
FF7	1	1	1	64	0.272	241	0.182
FF8	−1	−1	−1	90	0.196	235	0.078
FF9	0	0	0	82	0.219	301	0.195
FF10	1	−1	−1	84	0.205	253	0.032
FF11	−1	1	1	107	0.297	276	0.235
FF12	−1	1	−1	156	0.308	275	0.145
FF13	1	−1	1	65	0.378	248	0.066
FF14	1	−1	−1	97	0.246	268	0.045
FF15	−1	−1	−1	84	0.173	239	0.094
FF16	0	0	0	75	0.224	305	0.253
FF17	0	0	0	84	0.250	317	0.118
FF18	1	1	1	55	0.307	224	0.203
FF19	0	0	−1	77	0.242	308	0.241
FF20	0	0	0	84	0.251	337	0.171
FF21	−1	−1	1	69	0.343	233	0.124

(version 17) was used for all data analysis. Analysis of variance (ANOVA) was used for this purpose.

Once the models were obtained taking into account significant factors and interactions, a set of selected size-tuned vesicles were prepared and characterized.

2.3. Vesicle Preparation. For liposome preparation, appropriate weighed amounts of PC were dissolved in different volumes of absolute ethanol (5–20 mL range). The same procedure was applied to niosome preparation by weighing and dissolving S60 and Cho in a 1:0.5 weight ratio. Then, the organic solution was injected, with a syringe pump (KD Scientific, Holliston, MA) at a flow rate of 120 mL/h, into Milli-Q water that was kept at 60 °C and stirred at 500 rpm. Once vesicles formed, ethanol was removed at 40 °C under reduced pressure (90 kPa) in a rotary evaporator. The resulting vesicular systems were further sonicated for 15 min (CY-500 sonicator, Optic Ivymen System, Biotech SL, Barcelona, Spain), using an amplitude of 30–55%, a power of 500 W, and a frequency of 20 kHz. The sonication probe was placed in a 100 mL glass beaker at a constant depth, 1.5 cm above the container bottom.

2.4. Vesicle Characterization. **2.4.1. Vesicle Size.** The Z-average size and PDI of vesicles were determined by dynamic light scattering (DSL) using a Zetasizer Nano ZS system (Malvern Instruments Ltd., Malvern, U.K.). Three independent samples were taken from each formulation, and measurements

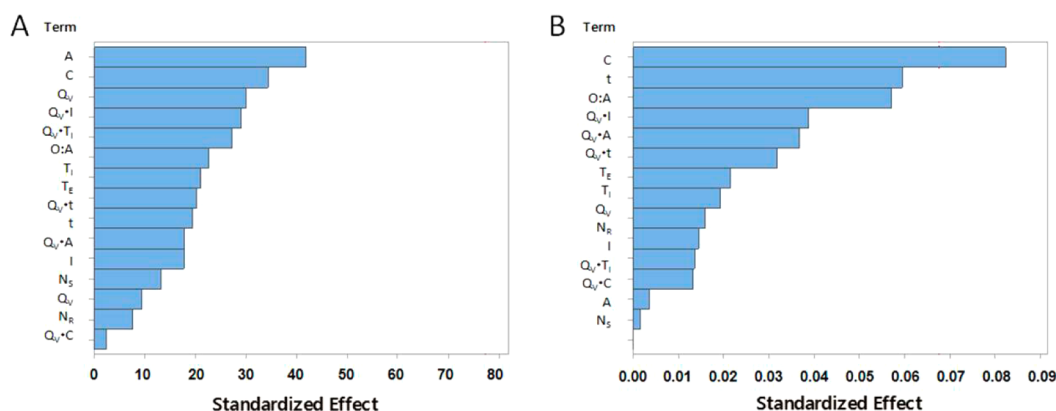


Figure 1. Pareto chart of the standardized effects of independent variables (factors) on the (A) Z-average size and (B) PDI of PC liposomes for the Plackett–Burman fractional factorial design.

232 were performed three times at room temperature without
233 dilution.

234 **2.4.2. Vesicle Morphology.** Morphological analysis of vesicles
235 was carried out by negative staining transmission electron
236 microscopy (NS-TEM), using a JEOL-2000 Ex II transmission
237 electron microscope (Tokyo, Japan). A sample drop was placed
238 on a carbon-coated copper grid, and excess sample was removed
239 with filter paper. Then, a drop of 2% (w/v) phosphotungstic acid
240 (PTA) solution was applied to the carbon grid and allowed to
241 stand for 1 min. Once the excess staining agent had been
242 removed with filter paper, the sample was air-dried, and the thin
243 film of stained and fixed vesicles was observed with the
244 transmission electron microscope.

245 **2.4.3. Vesicle Stability.** Vesicle stability was determined by
246 measuring backscattering (BS) profiles in a Turbiscan Lab Expert
247 apparatus (Formulation, L'Union, France) provided with an
248 aging station (Formulation, L'Union, France).

249 Samples were placed in cylindrical glass test cells, and
250 backscattered light was monitored at 30 °C as a function of
251 time and cell height every 2 h for 7 days.

252 The optical reading head scans the sample in the cell,
253 providing BS data every 40 μm in percentages relative to
254 standards as a function of the sample height (in millimeters).
255 These profiles build up a macroscopic fingerprint of the sample at
256 a given time, providing useful information about changes in the
257 size distribution or appearance of a creaming layer or a
258 clarification front with time.^{3,37,38}

259 **2.4.4. Encapsulation Efficiency (EE).** EE also provides useful
260 information related to the stability of the vesicle membrane.
261 Hydrophilic compounds are entrapped in aqueous compart-
262 ments between bilayers, whereas lipophilic compounds are
263 preferentially located within the surfactant or lipid bilayer.³⁹
264 Substances such as drugs, bioactive compounds, dyes, and
265 nanomaterials incorporated into vesicles can also affect the
266 morphology and stability of the final dispersion.

267 For the purpose of determining EEs, Sudan Red 7B and
268 vitamin D₃ (hydrophobic compounds) were encapsulated in the
269 two different formulations.

270 Each compound was analyzed by reverse-phase high-perform-
271 ance liquid chromatography (RP-HPLC) (HP series 1100
272 chromatograph, Hewlett-Packard, Palo Alto, CA). Before RP-
273 HPLC analysis could be performed, the nonencapsulated
274 compound had to be removed by passing the sample through a
275 Sephadex G-25 column (GE Healthcare Life Sciences,
276 Wauwatosa, WI). Then, both filtered and nonfiltered samples
277 were diluted 1:10 (v/v) with methanol to facilitate vesicle

rupture and to extract the encapsulated compound. EE was
278 calculated according to the equation
279

$$EE (\%) = \frac{\text{peak area of filtered sample}}{\text{peak area of unfiltered sample}} \times 100 \quad (1) \quad 280$$

The RP-HPLC system was equipped with an HP G1315A UV/
281 vis absorbance detector (Agilent Technologies, Palo Alto, CA).
282 The column was a Zorbax Eclipse Plus C18 column with a
283 particle size of 5 μm, 4.6 mm × 150 mm (Agilent Technologies,
284 Palo Alto, CA). The mobile phase consisted of a mixture of (A)
285 100% Milli-Q-water and (B) 100% methanol with gradient
286 elution at 0.8 mL/min. The step gradient started with a mobile
287 phase of 80% A, running 100% mobile phase B starting in minute
288 5 for 10 min. Mobile phase B was fed for 2 min after each
289 injection to prepare the column for the next sample. The
290 separation was carried out at 30 °C. Different wavelengths were
291 used for the UV/vis detector, namely, 533 nm for Sudan Red 7B
292 and 270 nm for vitamin D₃.
293

3. RESULTS AND DISCUSSION

3.1. Effects of Variables on Morphological Character-
294 **istics.** The responses (Z-average size and PDI) of each batch
295 from P–B design were measured by dynamic light scattering
296 (DLS). The relative importance of the main effects on the Z-
297 average size and PDI of PC liposomes are shown in the Pareto
298 chart given in Figure 1.
299

Researchers must be aware of the confusion of main effects
300 with two-factor interactions in this type of design (resolution III),
301 where the alias structure is too complex. However, we decided to
302 use the initial Plackett–Burman design only for screening
303 purposes and selection of the main factors from the Pareto chart,
304 as is usually accepted. Effects were selected by applying the
305 hierarchical ordering principle, known sometimes as the sparsity-
306 of-effects principle, where higher-order effects (three- or four-
307 way interactions) are sacrificed to study lower-order effects
308 (main effects first and two-way interactions next). This principle
309 suggests that priority should be given to the estimation of lower-
310 order effects, especially when resources (time and money) are
311 scarce. This postulate is an empirical principle whose validity has
312 been confirmed by the analysis of many real experiments.
313

According to these data, the most important variables for both
314 responses are the organic/aqueous phase volume ratio, the (final
315 aqueous-phase) phospholipid concentration, and the sonication
316 amplitude. These results are in good agreement with previous
317 studies carried out by Kremer et al.,⁴⁰ who evaluated the effects of
318

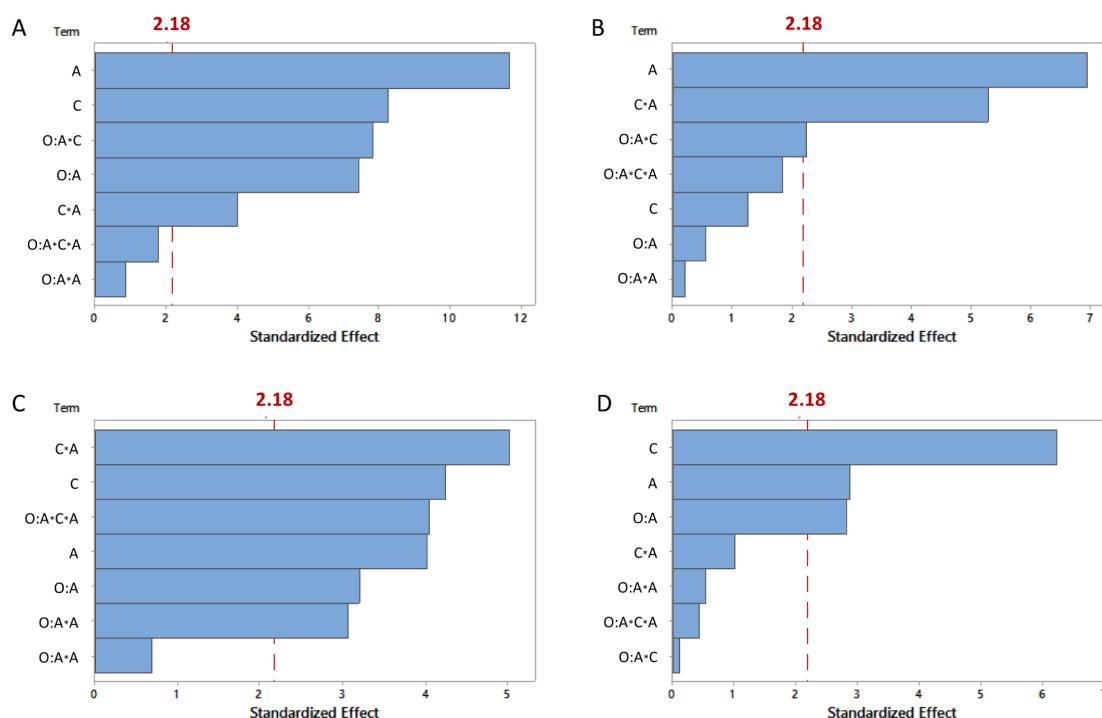


Figure 2. Pareto chart of the standardized effects of independent variables (factors) on the (A,C) Z-average size and (B,D) PDI of (A,B) PC liposomes and (C,D) S60:Cho niosomes (1:0.5, w/w) for the 2^3 full factorial design.

319 some preparation variables on the size and polydispersity of
 320 liposomes made from two different natural phosphatidylcholines.
 321 Their experimental results showed that the most important
 322 factor in the final size of the liposomes was the lipid
 323 concentration in the alcohol injected into the buffer solution.
 324 This factor corresponds to the interaction of the lipid amount
 325 and the flow rate of organic solvent injected, two factors present
 326 in the Pareto chart in Figure 1. The same explanation was
 327 postulated by other authors,^{8,41,42} confirming that the lipid
 328 concentration clearly affects the liposome size. This factor was
 329 found to be the most relevant one for controlling morphological
 330 characteristics of phosphatidylcholine liposomes. Szoka⁴³ found
 331 that stirring, ionic strength, and temperature of the aqueous
 332 phase could also contribute to the final size, but the effects of
 333 these factors were smaller than those observed for lipid
 334 concentration, organic/aqueous phase ratio, and chemical nature
 335 of the organic solvent (a parameter not included in our study).
 336 Therefore, the experimental results in Figure 1 confirm the
 337 previously reported observations.⁴³

338 The ethanol injection method is usually chosen because it
 339 avoids the sonication step, which is needed in several other
 340 methods of liposome preparation, such as the thin-film hydration
 341 method. Preliminary experiments (data not shown) indicated
 342 that sonication is a crucial step for reducing the size of both
 343 liposomes and niosomes. Alternatively, small vesicles can be
 344 produced without sonication by using low concentrations of
 345 lipids/surfactants, but with low yield. This is why we decided to
 346 include this step as a factor in the present study.

347 **3.2. PC Liposomes.** The first three main effects from the
 348 Pareto chart obtained for the P–B design were selected for the 2^3
 349 full factorial design. The ANOVA results for Z-average size and
 350 PDI values are listed in Tables S1 and S2 (Supporting
 351 Information), respectively, whereas the corresponding Pareto
 352 chart is shown in Figure 2. Mean sizes in the range of 55–156 nm
 353 with PDI values between 0.173 and 0.378 were obtained for PC

liposomes (with standard deviations ranging from 0.304 to 4.40
 354 nm for size and from 0.003 to 0.053 for PDI). Similar size ranges
 355 were also obtained using the EIM in other previously reported
 356 studies.^{22,27,41,43,44}

357 The normality, variance homogeneity, and randomness
 358 assumptions were tested with a normal probability plot,
 359 frequency histogram, and residuals versus fits and residuals
 360 versus order plots, respectively (Supporting Information, Figure
 361 S2).

362 No clear aberrant tendencies were observed, because the
 363 residuals tended to form a line, no typical cornet pattern was
 364 observed, and no time-based pattern was detected. Only some
 365 outlier values were detected (Cook's distance and DFITS values
 366 are given in Table S3 of the Supporting Information).

367 The ANOVA results allowed for an analysis of the
 368 contributions of the effects of the independent variables on the
 369 response function (mean size of PC liposomes). In this case,
 370 significant two-way interactions were identified: (O/A) \times C and
 371 C \times A (see Figure 3). Larger sizes are reached when the organic
 372 solution has a higher lipid concentration (more than 20 g/L). On
 373 the other hand, the C \times A interaction reveals that the degree of
 374 size reduction upon application of a higher amplitude depends
 375 on the total lipid concentration present in the medium (referred
 376 to the final volume of the dispersion).

377 All of the main effects are significant ($p < 0.05$), with a positive
 378 effect on the mean size (a higher response value with an increase
 379 in the factor level) for the total lipid concentration and a negative
 380 effect (a lower response value with a decrease in factor level) for
 381 the organic/aqueous phase volume ratio and the sonication
 382 amplitude.

383 These effects can be explained according to a previously
 384 reported vesicle formation model.^{45–47} This model relies on the
 385 formation of vesicles through intermediate structures, such as
 386 phospholipid bilayer fragments and sheet-like micelles. These
 387

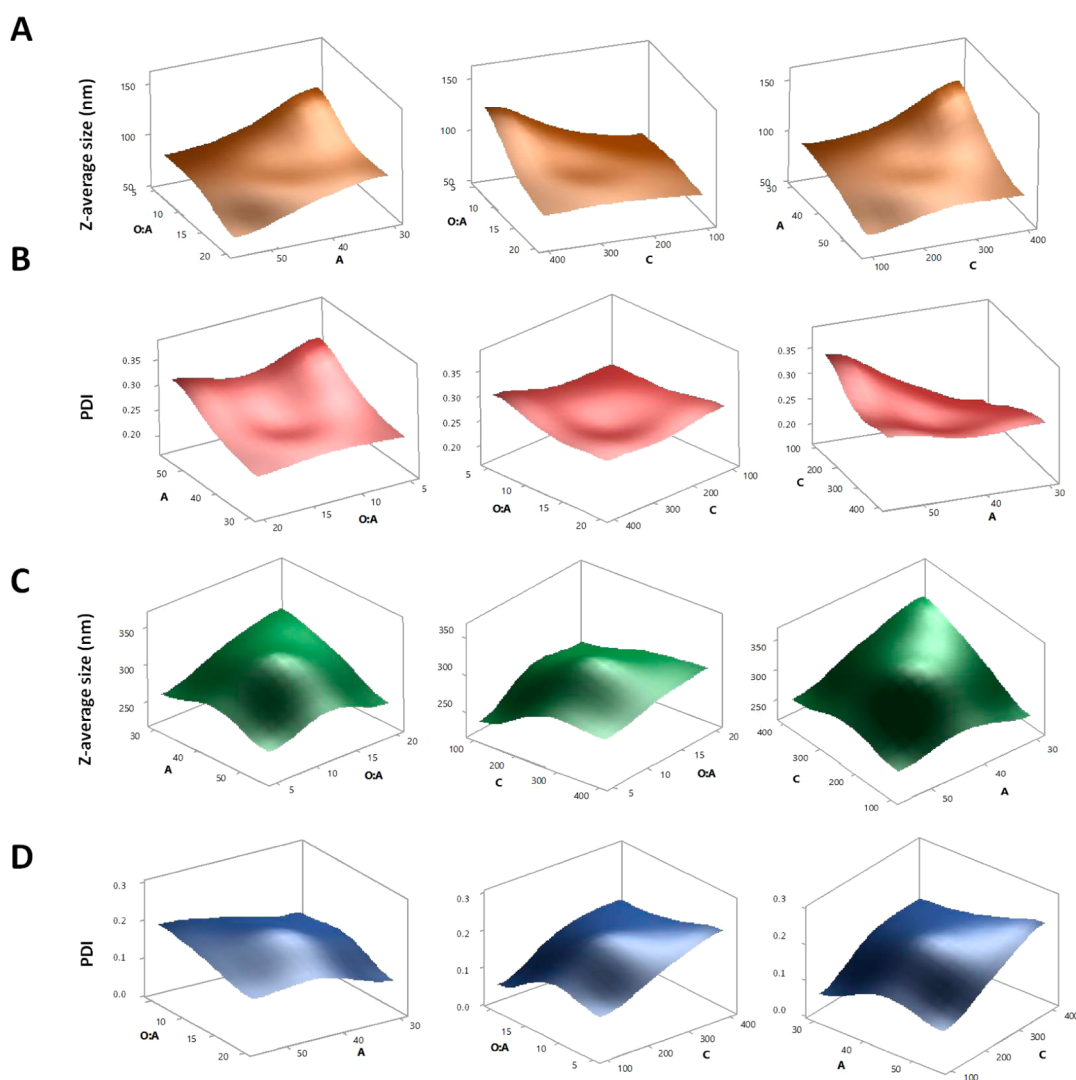


Figure 3. Three-dimensional (3D) response surface plots for the factors O/A (organic/aqueous phase volume ratio), C (lipid or surfactant/stabilizer concentration, g/L), and A (sonication amplitude, %) for the (A,C) Z-average size and (B,D) PDI of (A,B) PC liposomes and (C,D) S60:Cho niosomes (1:0.5, w/w).

intermediates are the result of amphiphilic self-assembly because of their characteristic physicochemical properties.⁴⁸

During the injection of ethanol droplets into the aqueous phase, lipid reorganization inside these dispersed droplets to form bilayers is favored by the fact that lipids energetically prefer a parallel molecular arrangement.⁴⁵ These planar structures give rise to closed vesicles when their size induces enough surface tension to close the structure and minimize the bending energy. The sizes of these intermediates depend directly on the number of lipid molecules (concentration) and the dispersion degree (solubilization) in the organic phase. It is obvious from the previous assessment that higher concentrations of lipids in the droplets will form higher membrane fragments, as our experimental results and previous observations confirm.^{8,40–42}

It is also important to know how easily lipid droplets are dispersed, as well as their size and homogeneity. Lipids of higher solubility will then form smaller lipid droplets and, consequently, shorter membrane fragments (and ultimately tiny vesicles).⁴⁰ This explains, in a simplified way, why higher organic/aqueous phase ratios yield smaller liposomes.

The negative effect of the sonication amplitude is explained by vesicle rupture, which takes place when an excess of energy is

applied to vesicles during the sonication process as a result of the effect of induced cavitation.^{49,50} The final effect of ultrasounds can be controlled by varying the input power, ultrasound frequency, sonication time, and probe depth into the container. As frequency increases, liposomes of smaller size are produced as a result of stronger acoustic cavitation events. This assumption was confirmed by our results, in accordance with previous studies.^{49,50} It is important to point out that, to minimize the effects of variations in the probe depth, this factor was kept constant at 1.5 cm above the container bottom.

Another aspect to be taken into consideration is the effect of sonication time. It was reported by Silva et al.⁴⁹ that sonication time plays an important role in decreasing vesicle size, although they observed that this effect reached a plateau at about 21 min. Our P–B design revealed a positive effect of sonication time on the Z-average size (from 15 to 30 min), although it was weaker than the effects of the other variables selected for the 2³ full factorial design (especially sonication amplitude). A similar influence was observed for the PDI response, but with a stronger effect. We preferred to select sonication amplitude instead of sonication time because one of the goals of controlling factors is to obtain a narrow size distribution.

Table 3. Estimated Coded Coefficients for the Considered Effects on the Z-Average Size and PDI of PC Liposomes and S60:Cho Niosomes (1:0.5, w/w)

response	coefficients ^a								R ²
	constant	X ₁	X ₂	X ₃	X ₁ X ₂	X ₁ X ₃	X ₂ X ₃	X ₁ X ₂ X ₃	
	Z-Average Size								
liposome (Y ₁)	89.68	-11.14	12.40	-17.50	-11.75	-	-5.97	-	96.69
niosome (Y ₃)	269.82	12.72	16.87	-15.94	-	-12.15	-19.92	-16.04	91.27
	PDI								
liposome (Y ₂)	0.280	-	-	0.038	-0.012	-	-0.029	-	89.35
niosome (Y ₄)	0.136	-0.026	0.057	0.026	-	-	-	-	84.73

^aX₁, organic/aqueous phase volume ratio; X₂, PC or S60:Cho concentration (g/L); X₃, sonication amplitude (%).

432 As the design included a center point with several repetitions
433 ($n = 5$), the presence of curvature in the response variables could
434 be tested (Figure 3). Because curvature seemed to be significant
435 ($p < 0.05$), a term involving center point (Ct Pt) was included in
436 the equations for its estimation.

437 With all of this information about the effects and their
438 estimated coefficients, the following equation ($R^2 = 96.69\%$) for
439 the Z-average size value of PC liposomes (Y₁) was generated

$$Y_1 = 62.8 + 2.55(O/A) + 0.449C - 0.185A - 0.0185(O/A) \times C - 0.00555C \times A - 9.26(\text{Ct Pt}) \quad (2)$$

441 Different behavior was observed regarding PDI, which was
442 strongly affected by the sonication amplitude as the only
443 significant main effect and its interaction with the total lipid
444 amount. The O/A × C interaction was also detected, but with a
445 lower effect on the PDI response.

446 To understand the C × A interaction, it is important to take
447 into account the effect of the sonication amplitude as the main
448 effect. An increase in this factor leads to a less monodisperse size
449 distribution, that is, higher PDI values. However, according to
450 the interaction, this response depends highly on the total amount
451 of lipids present in the sample. At a low level of the lipid amount,
452 the reduction in size is more effective (as previously mentioned),
453 but the size distribution is large. However, at a high level of the
454 lipid amount, this enlargement of the size distribution is
455 significantly lower.

456 Curvature in the response was also tested, again revealing a
457 significant presence ($p < 0.05$). For the PDI response (Y₂), the
458 following equation with an R² value of 89.35% was obtained

$$Y_2 = -0.160 + 0.00939A - 0.0000420(O/A) \times C - 0.0000250C \times A - 0.0425(\text{Ct Pt}) \quad (3)$$

460 These equations were formulated with uncoded coefficients,
461 making it easier to use them to predict selected target size and
462 PDI values.

463 **3.3. S60:Cho Niosomes.** To investigate whether the
464 selected factors in the P–B design for PC liposomes (a reference
465 model for vesicular systems) produced similar effects with other
466 different formulations, the same 2³ full factorial design using
467 center-point replicates was performed for a typical niosome
468 formulation, in this particular case, S60:Cho niosomes (1:0.5, w/
469 w). The main variables were the organic/aqueous phase volume
470 ratio (O/A), the total concentration of surfactant and stabilizer
471 (C), and the sonication amplitude (A).

472 The ANOVA results for Z-average size and PDI values are
473 listed in Table S1 (Supporting Information), and the
474 corresponding Pareto chart and three-dimensional surface plot

are shown in Figures 2 and 3, respectively. Mean sizes in the
range of 224–362 nm with PDI values between 0.032 and 0.291
were obtained for S60:Cho niosomes (with standard deviations
ranging from 1.05 to 7.28 nm for size and from 0.009 to 0.052 for
PDI). Similar size and PDI ranges were reported for niosomes
prepared by the EIM using Span 60 as the membrane
component.¹⁷

Two-way interactions (O/A × A, C × A) and a three-way
interaction (O/A × C × A) were detected, with sonication
amplitude (A) as the common factor in these interactions (see
Figure 2C). Therefore, it can be postulated that sonication
amplitude is the key factor in the niosome size response. The
response depends on both the O/A and C factor levels, with a
higher interaction between the sonication amplitude and the
total amount of membrane components. Differences in the
magnitude of the coefficient of this factor between liposomes and
niosomes can be attributed to the initial size before sonication
(smaller for liposomes) and vesicle stability.⁵⁰

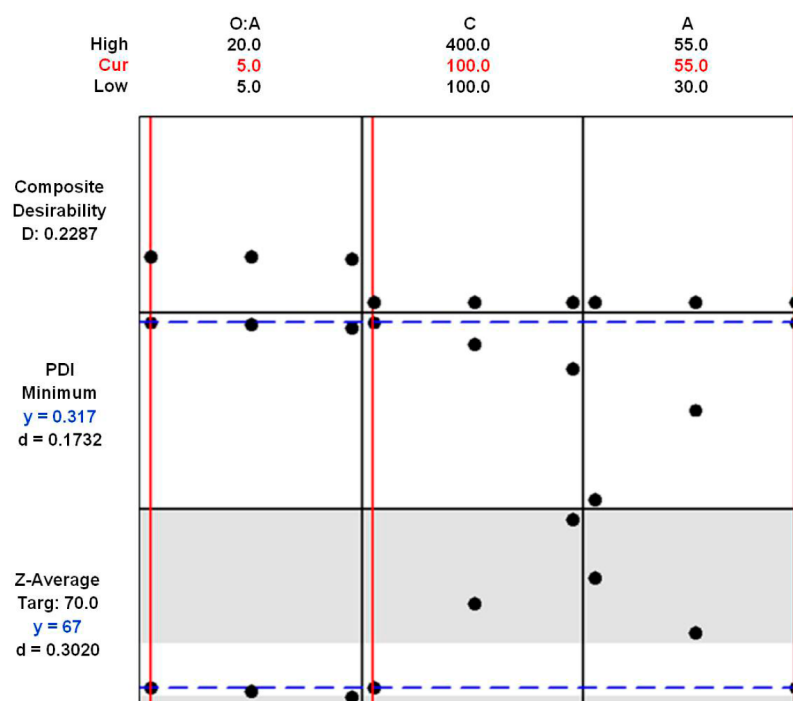
The three main effects are significant, but in contrast to the
case for liposomes, the organic/aqueous phase volume ratio (O/
A) shows a positive effect on niosome size. This behavior could
be due to different molecular features of the surfactant and
stabilizer that result in different interactions with the organic
phase and, therefore, poor or insufficient solubility.

The other two variables (C, A) have effects similar to those
described above for liposomes. Therefore, the same explanation
regarding surfactant concentration and sonication amplitude can
be applied here to justify their effects on niosome size. In this
case, the stronger effect of C is explained by the influence of
cholesterol on the final size of vesicles, as reported by Padamwar
and Pokharkar.⁸

Once again, curvature was detected for the Z-average size
response. The following equation was obtained to model this
case, with an adjusted correlation coefficient (R²) of 91.27%

$$Y_3 = 236.9 - 4.31(O/A) - 0.012C - 0.56A + 0.0461(O/A) \times C + 0.00363C \times A - 0.00114(O/A) \times C \times A + 44.00(\text{Ct Pt}) \quad (4)$$

On the other hand, a completely different behavior was observed
regarding the PDI response. Only the three main effects (O/A, C,
A) were found to be significant, and no interactions were found.
Two positive effects on the niosome PDI were detected:
surfactant/stabilizer concentration and sonication amplitude. In
this case, the total concentration of membrane components
seemed to have an important role in the vesicle size distribution,
as can be seen in the correspondent Pareto chart (Figure 2). This
observation once again can be attributed to the solubilization of
membrane components in the organic phase. Higher concen-



Parameters

Response	Goal	Lower	Target	Upper	Weight	Importance
Z-Average PC-Liposomes	Target	65	70.000	75.000	1	1
PDI PC-Liposomes	Minimum		0.173	0.378	1	1

Solution

Solution	O:A	C	A	Z-Average PC-Liposomes Fit	PDI PC-Liposomes Fit	Composite Desirability
1	5	100	55	67	0.317	0.2287

Response	Fit	SE Fit	95% CI	95% PI
Z-Average PC-Liposomes	67	4	(57, 76)	(51, 83)
PDI PC-Liposomes	0.317	0.013	(0.308, 0.377)	(0.284, 0.402)

Figure 4. Optimization plot and values of individual (d) and composite (D) desirability provided by the response optimizer (Minitab, version 17) for an example of size-tuned PC liposome (desired size = 70 nm, with a minimum PDI value).

520 trations of these components require better solubilization in
521 dispersed droplets to reach small membrane fragments.

522 It is important to note that some combinations of factors
523 yielded narrow size distributions, namely, $PDI \leq 0.100$, a value
524 frequently obtained by other preparation methods, such as
525 microfluidic hydrodynamic focusing⁵¹ also using S60:Cho as the
526 formulation.

527 A negative effect was detected for the organic/aqueous phase
528 volume ratio (O/A). As the final concentration of ethanol
529 increased during the injection process, a smaller size distribution
530 was obtained. As previously mentioned, no interaction between
531 this factor and the total concentration of membrane components
532 was observed.

533 The following equation with an R^2 value of 84.73% was
534 obtained for the niosome PDI model response (Y_4)

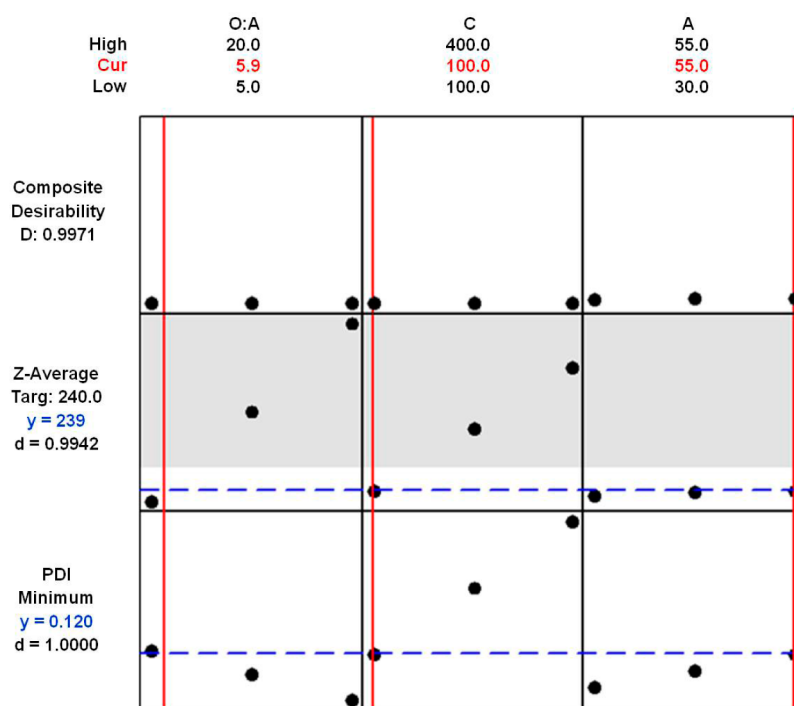
$$Y_4 = 0.053 - 0.00392(O/A) + 0.000039C + 0.00067A + 0.0597(Ct Pt) \quad (5)$$

535

The estimated coded coefficients for the considered effects on the Z-average sizes and PDIs of PC liposomes and S60:Cho niosomes are listed in Table 3, as a summary of the factors' influence. Coded coefficients were used to maintain the orthogonality of the designs and to allow for a direct comparison between coefficients.

3.4. Vesicle Characterization. Size-tuned vesicles were prepared under selected operating conditions by applying the models obtained from the experimental design (eqs 2–5) and the assistance of the response optimizer and response predictor in Minitab statistical software (version 17). These tools can be applied to the simultaneous optimization of several responses only when the same set of factors are studied separately, because a common experimental region is needed.

The operating conditions were selected to prepare PC liposomes with a mean size of 70 nm and the minimum PDI value (predicted values of $Y_1 = 67 \pm 4$ and $Y_2 = 0.317 \pm 0.013$) and S60-Cho niosomes with a mean size of 240 nm and the



Parameters

Response	Goal	Lower	Target	Upper	Weight
Z-Average S60:Cho Niosomes	Target	235	240.000	245.000	1
PDI S60:Cho Niosomes	Minimum		0.120	0.291	1

Solutions

Solution	O:A	C	A	PDI S60:Cho Niosomes Fit	Z-Average S60:Cho Niosomes Fit	Composite Desirability
1	5.9	100	55	0.120	239	0.9971

Response	Fit	SE Fit	95% CI	95% PI
Z-Average S60:Cho Niosomes	239	11	(217, 263)	(198, 281)
PDI S60:Cho Niosomes	0.120	0.025	(0.066, 0.172)	(0.024, 0.214)

Figure 5. Optimization plot and values of individual (d) and composite (D) desirability provided by the response optimizer (Minitab, version 17) for an example of size-tuned S60:Cho niosome (1:0.5 w/w) (desired size = 240 nm, with a minimum PDI).

554 minimum PDI value (predicted values of $Y_3 = 239 \pm 11$ and $Y_4 =$
555 0.120 ± 0.025). These sizes and PDI values were selected only as
556 an example. The factor output values were O/A = 5:50, C = 2 g/
557 L, and A = 55% for the liposomes and O/A = 5.9:50, C = 2 g/L,
558 and A = 55% for the niosomes. Figures 4 and 5 show optimization
559 plots and values of individual and composite desirability for size-
560 tuned liposomes and size-tuned niosomes, respectively.

561 The experimental results showed that the models obtained
562 with the experimental design were accurate, because mean sizes
563 of 69 ± 0.5 nm (PDI = 0.245 ± 0.005) and 233 ± 3 nm (PDI =
564 0.112 ± 0.004) were obtained for the PC liposomes and S60:Cho
565 niosomes, respectively. The relative error was low for the
566 experimental results regarding mean size (3% for Y_1 and Y_3) but
567 higher for the size distributions (22% for Y_2 and 7% for Y_4).

568 The sizes and morphologies of the vesicles were investigated
569 by TEM, using a negative contrast. Figure 6 shows black-stained

570 vesicles, as a result of the interactions of the electron beam with
571 PTA, which produces a selective deposit of metal ions that
572 enhances morphological details. The micrographs show spherical
573 structures of approximately 80 nm for the liposomes (Figure 6C)
574 and about 250 nm for the niosomes (Figure 6D). These values
575 agree with the DLS measurements.

576 Figure 6D shows clusters of niosomes that are all similar in
577 size. Aggregation arose during the drying step prior to TEM
578 measurements, because no flocculation phenomena were
579 monitored with the Turbiscan apparatus.

580 Slight differences were noticed in the zeta potential measure-
581 ments, exhibiting low values for both types of vesicles. Niosomes
582 had values of about -16.8 ± 0.7 mV, whereas the liposomes had
583 values of -6.9 ± 0.3 mV. This small value for the liposomes could
584 be due to neutralization of the negative charge from the

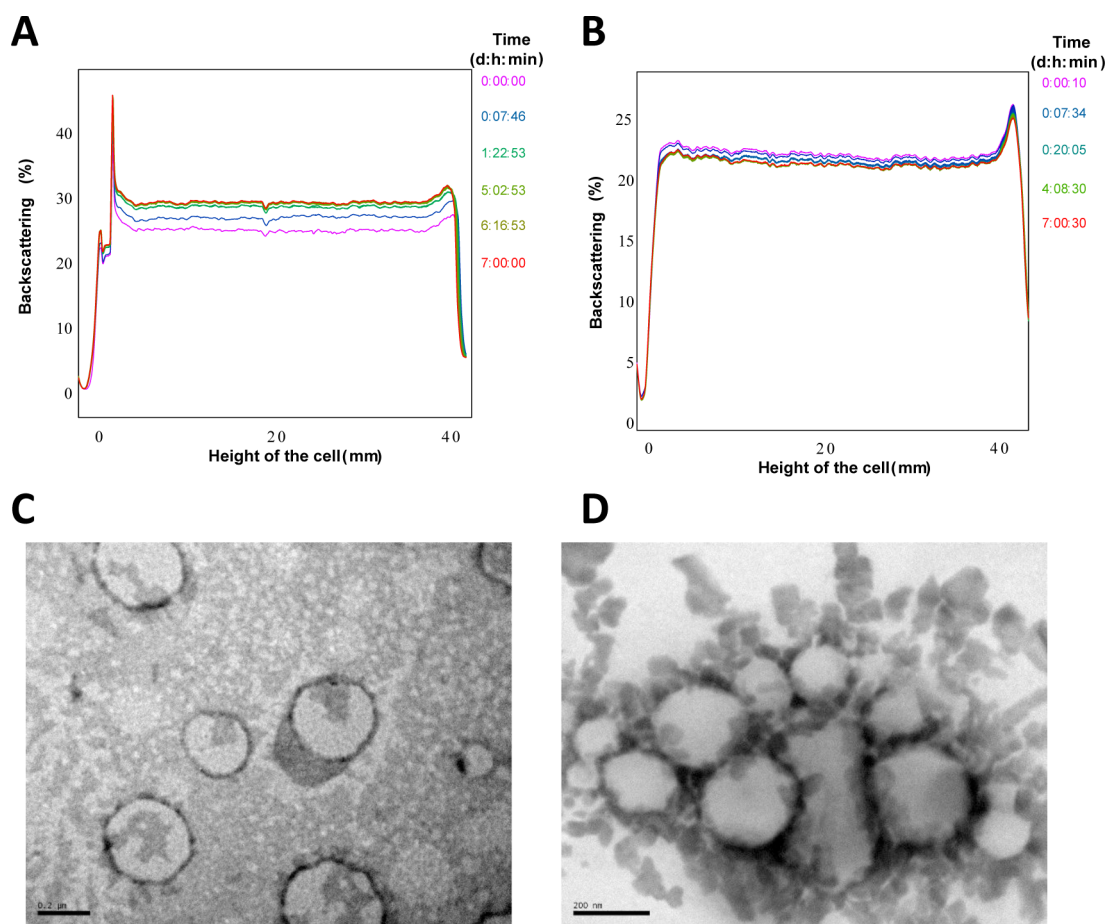


Figure 6. (A,B) BS profiles and (C,D) TEM micrographs of empty vesicles designed with a controlled size and PDI values by applying the models obtained from experimental design: (A,C) PC liposomes and (B,D) S60:Cho niosomes (1:0.5, w/w).

585 phosphate groups by sodium cations present in the medium
586 (from sodium chloride in the PB solution).

587 The formulated vesicles exhibited a high stability after 1 week
588 of monitoring time. BS profiles obtained for the PC liposomes
589 are given in Figure 6, where a variation of 4.5% in the middle part
590 of the cell (from 10 to 30 mm) is noticed. A simultaneous slight
591 clarification process was observed in the middle and top parts of
592 the cell in the corresponding transmission profile (results not
593 shown). This was promoted by some movement of the PC
594 liposomes toward the bottom of the cell, resulting in a slight
595 increase in BS (sedimentation). However, this was a reversible
596 process, caused by differences in concentration, with the sample
597 remaining stable and maintaining its initial properties (size and
598 PDI). The vesicles were again characterized after gentle agitation
599 of the cell at the end of the monitoring time with analogous
600 results.

601 For the S60:Cho niosomes (Figure 6B), the BS profile
602 remained nearly constant (variations of approximately 0.5%)
603 with time, showing high stability. Some variation was also
604 observed in the transmission profile all along the cell height,
605 because the sample was not translucent.

606 **3.4.1. Encapsulation Efficiency (EE).** Vesicles containing
607 Sudan Red 7B and vitamin D₃ as model compounds (both
608 lipophilic) were also prepared and characterized. No differences
609 were observed regarding mean size and PDI values or TEM, zeta
610 potential, or Turbiscan measurements, meaning that the
611 entrapped compounds did not affect the vesicle's behavior.

High EE values were obtained for both Sudan Red 7B and 612
vitamin D₃, as expected taking into account their hydrophobic 613
character. EE values up to 90.1% and 88.0% were obtained for 614
Sudan Red 7B encapsulated in PC liposomes and S60:Cho 615
niosomes, respectively. Experiments carried out with vitamin D₃ 616
led to EE values of 99.2% for PC liposomes and 73.9% for 617
S60:Cho niosomes. These results are in good agreement with 618
those of previous studies, where compounds with similar 619
chemical properties were encapsulated.^{12,13,27} 620

4. CONCLUSIONS

In this work, an adequate approximation using DoE was applied 621
to study the influence of experimental factors of the EIM on the 622
mean size and size distribution of PC liposomes and S60:Cho 623
niosomes (1:0.5, w/w). 624

An initial screening design enabled a reduction of the number 625
of variables. This was a necessary step before carrying out a full 626
factorial design. Finally, response models were applied to prepare 627
selected size-tuned nanovesicles, which were characterized from 628
a stability point of view. 629

This was achieved with a low number of experiments (58 630
runs). This methodology enabled two different formulations 631
(liposomes and niosomes, the most common types of nano- 632
vesicles) to be studied in a comparative way. Stable liposomes 633
and niosomes of the targeted sizes were successfully prepared 634
with the model equations obtained, with encapsulation 635
efficiencies higher than 73.9% in all cases for selected 636
hydrophobic compounds. 637

638 The most important variables identified by ANOVA were the
639 organic/aqueous phase volume ratio, the (final aqueous-phase)
640 phospholipid concentration, and the sonication amplitude.
641 These results offer new insights into the mechanism and effects
642 of the factors involved in nanovesicle preparation by the EIM,
643 one of the most easily scaled-up methods for preparing vesicles
644 for several fields of interest.

645 ■ ASSOCIATED CONTENT

646 ● Supporting Information

647 The Supporting Information is available free of charge on the
648 ACS Publications website at DOI: 10.1021/acs.iecr.6b01552.

649 ANOVA results for Z-average size and PDI of PC
650 liposomes for the 2³ full factorial design; Cook's distances
651 and DFITS values for each response in the full factorial
652 designs; optimization contour plot for the factors studied
653 in the full factorial design for both responses; testing for
654 normality, variance homogeneity, and randomness
655 assumptions of ANOVA for the full factorial design
656 (PDF)

657 ■ AUTHOR INFORMATION

658 Corresponding Author

659 *Tel.: +34 985103509. E-mail: cpazos@uniovi.es.

660 Notes

661 The authors declare no competing financial interest.

662 ■ ACKNOWLEDGMENTS

663 This work was supported by the Ministerio de Economía y
664 Competitividad (MINECO, Spain), under Grant MINECO-13-
665 CTQ2013-47396-R. This study was also cofinanced by the
666 Consejería de Educación y Ciencia del Principado de Asturias
667 (ref FC-04-COF-50-MEC, PCTI Asturias 2006-2009, ref
668 EQP06-024, and FC15-GRUPIN14-022). We especially thank
669 Prof. Antonia Salas (University of Oviedo) for her advice with
670 the statistical work.

671 ■ REFERENCES

672 (1) Capretto, L.; Carugo, D.; Mazzitelli, S.; Nastruzzi, C.; Zhang, X.
673 Microfluidic and lab-on-a-chip preparation routes for organic nano-
674 particles and vesicular systems for nanomedicine applications. *Adv. Drug*
675 *Delivery Rev.* **2013**, *65*, 1496–1532.
676 (2) Rongen, H. A. H.; Bult, A.; van Bennekom, W. P. Liposomes and
677 immunoassays. *J. Immunol. Methods* **1997**, *204*, 105–133.
678 (3) Pando, D.; Gutiérrez, G.; Coca, J.; Pazos, C. Preparation and
679 characterization of niosomes containing resveratrol. *J. Food Eng.* **2013**,
680 *117*, 227–234.
681 (4) Gómez-Hens, A.; Fernández-Romero, J. M. The role of liposomes
682 in analytical processes. *TrAC, Trends Anal. Chem.* **2005**, *24*, 9–19.
683 (5) Edwards, K. A.; Bolduc, O. R.; Baeumner, A. J. Miniaturized
684 bioanalytical systems: enhanced performance through liposomes. *Curr.*
685 *Opin. Chem. Biol.* **2012**, *16*, 444–452.
686 (6) Liu, Q.; Boyd, B. J. Liposomes in biosensors. *Analyst* **2013**, *138*,
687 391–409.
688 (7) Canton, I.; Battaglia, G. Endocytosis at the nanoscale. *Chem. Soc.*
689 *Rev.* **2012**, *41*, 2718–39.
690 (8) Padamwar, M. N.; Pokharkar, V. B. Development of vitamin loaded
691 topical liposomal formulation using factorial design approach: Drug
692 deposition and stability. *Int. J. Pharm.* **2006**, *320*, 37–44.
693 (9) Taha, E. I. Lipid vesicular systems: formulation optimization and ex
694 vivo comparative study. *J. Mol. Liq.* **2014**, *196*, 211–216.
695 (10) Abdelbary, A. A.; AbouGhaly, M. H. H. Design and optimization
696 of topical methotrexate loaded niosomes for enhanced management of

psoriasis: Application of Box–Behnken design, in-vitro evaluation and 697
in-vivo skin deposition study. *Int. J. Pharm.* **2015**, *485*, 235–243. 698
(11) Jadhav, S. M.; Morey, P.; Karpe, M.; Kadam, V. Novel vesicular 699
system: An overview. *J. Appl. Pharm. Sci.* **2012**, *02*, 193–202. 700
(12) Rajera, R.; Nagpal, K.; Singh, S. K.; Mishra, D. N. Niosomes: a 701
controlled and novel drug delivery system. *Biol. Pharm. Bull.* **2011**, *34*,
945–53. 702
(13) Uchegbu, I. F.; Vyas, S. P. Non-ionic surfactant based vesicles 703
(niosomes) in drug delivery. *Int. J. Pharm.* **1998**, *172*, 33–70. 704
(14) Bangham, A. D.; Standish, M. M.; Watkins, J. C. Diffusion of 705
univalent ions across the lamellae of swollen phospholipids. *J. Mol. Biol.*
1965, *13*, 238–252. 706
(15) da Silva Malheiros, P.; Daroit, D. J.; Brandelli, A. Food 707
applications of liposome-encapsulated antimicrobial peptides. *Trends*
Food Sci. Technol. **2010**, *21*, 284–292. 708
(16) du Plessis, J.; Weiner, N.; Müller, D. G. The influence of in vivo 709
treatment of skin with liposomes on the topical absorption of a 710
hydrophilic and a hydrophobic drug in vitro. *Int. J. Pharm.* **1994**, *103*,
R1–R5. 711
(17) Manconi, M.; Sinico, C.; Valenti, D.; Loy, G.; Fadda, A. M. 712
Niosomes as carriers for tretinoin I: Preparation and properties. *Int. J.*
Pharm. **2002**, *234*, 237–248. 713
(18) Manca, M. L.; Manconi, M.; Nacher, A.; Carbone, C.; Valenti, D.; 714
Maccioni, A. M.; Sinico, C.; Fadda, A. M. Development of novel 715
diolein–niosomes for cutaneous delivery of tretinoin: Influence of 716
formulation and in vitro assessment. *Int. J. Pharm.* **2014**, *477*, 176–186. 717
(19) Mahale, N. B.; Thakkar, P. D.; Mali, R. G.; Walunj, D. R.; 718
Chaudhari, S. R. Niosomes: Novel sustained release nonionic stable 719
vesicular systems — An overview. *Adv. Colloid Interface Sci.* **2012**, *183–*
184, 46–54. 720
(20) Moghassemi, S.; Hadjizadeh, A. Nano-niosomes as nanoscale 721
drug delivery systems: An illustrated review. *J. Controlled Release* **2014**,
185, 22–36. 722
(21) Mali, N.; Darandale, S.; Vavia, P. Niosomes as a vesicular carrier 723
for topical administration of minoxidil: formulation and in vitro 724
assessment. *Drug Delivery Transl. Res.* **2013**, *3*, 587–592. 725
(22) Fan, M.; Xu, S.; Xia, S.; Zhang, X. Preparation of salidroside nano- 726
liposomes by ethanol injection method and in vitro release study. *Eur.*
Food Res. Technol. **2008**, *227*, 167–174. 727
(23) Marianecchi, C.; Di Marzio, L.; Rinaldi, F.; Celia, C.; Paolino, D.; 728
Alhaique, F.; Esposito, S.; Carafa, M. Niosomes from 80s to present: The 729
state of the art. *Adv. Colloid Interface Sci.* **2014**, *205*, 187–206. 730
(24) Akbarzadeh, A.; Rezaei-Sadabady, R.; Davaran, S.; Joo, S. W.; 731
Zarghami, N.; Hanifehpour, Y.; Samiei, M.; Kouhi, M.; Nejati-Koshki, K. 732
Liposome: classification, preparation, and applications. *Nanoscale Res.*
Lett. **2013**, *8*, 102. 733
(25) Justo, O. R.; Moraes, Â. M. Analysis of process parameters on the 734
characteristics of liposomes prepared by ethanol injection with a view to 735
process scale-up: Effect of temperature and batch volume. *Chem. Eng.*
Res. Des. **2011**, *89*, 785–792. 736
(26) Batzri, S.; Korn, E. D. Single bilayer liposomes prepared without 737
sonication. *Biochim. Biophys. Acta, Biomembr.* **1973**, *298*, 1015–1019. 738
(27) Pham, T. T.; Jaafar-Maalej, C.; Charcosset, C.; Fessi, H. Liposome 739
and niosome preparation using a membrane contactor for scale-up. 740
Colloid. Colloids Surf., B **2012**, *94*, 15–21. 741
(28) Loukas, Y. L. Experimental studies for screening the factors that 742
influence the effectiveness of new multicomponent and protective 743
liposomes. *Anal. Chim. Acta* **1998**, *361*, 241–251. 744
(29) Shah, S. R.; Parikh, R. H.; Chavda, J. R.; Sheth, N. R. Application 745
of Plackett–Burman screening design for preparing glibenclamide 746
nanoparticles for dissolution enhancement. *Powder Technol.* **2013**, *235*,
405–411. 747
(30) El-Samalgny, M. S.; Afifi, N. N.; Mahmoud, E. A. Increasing 748
bioavailability of silymarin using a buccal liposomal delivery system: 749
Preparation and experimental design investigation. *Int. J. Pharm.* **2006**,
308, 140–148. 750
(31) Shaikh, K. S.; Chellampillai, B.; Pawar, A. P. Studies on nonionic 751
surfactant bilayer vesicles of ciclopirox olamine. *Drug Dev. Ind. Pharm.*
2010, *36*, 946–53. 752
753
754
755
756
757
758
759
760
761
762
763
764
765

- 766 (32) Mahmood, S.; Taher, M.; Mandal, U. K. Experimental design and
767 optimization of raloxifene hydrochloride loaded nanotransfersomes for
768 transdermal application. *Int. J. Nanomed.* **2014**, *9*, 4331–4346.
- 769 (33) Chaudhary, H.; Kohli, K.; Kumar, V. Nano-transfersomes as a
770 novel carrier for transdermal delivery. *Int. J. Pharm.* **2013**, *454*, 367–380.
- 771 (34) Derakhshandeh, K.; Erfan, M.; Dadashzadeh, S. Encapsulation of
772 9-nitrocaptophecic, a novel anticancer drug, in biodegradable
773 nanoparticles: Factorial design, characterization and release kinetics.
774 *Eur. J. Pharm. Biopharm.* **2007**, *66*, 34–41.
- 775 (35) Alund, S. J.; Smistad, G.; Hiorth, M. A. A multivariate analysis
776 investigating different factors important for the interaction between
777 liposomes and pectin. *Colloids Surf, A* **2013**, *420*, 1–9.
- 778 (36) Gonzalez-Mira, E.; Egea, M. A.; Garcia, M. L.; Souto, E. B. Design
779 and ocular tolerance of flurbiprofen loaded ultrasound-engineered NLC.
780 *Colloids Surf, B* **2010**, *81*, 412–421.
- 781 (37) Pando, D.; Caddeo, C.; Manconi, M.; Fadda, A. M.; Pazos, C.
782 Nanodesign of olein vesicles for the topical delivery of the antioxidant
783 resveratrol. *J. Pharm. Pharmacol.* **2013**, *65*, 1158–1167.
- 784 (38) Pando, D.; Matos, M.; Gutiérrez, G.; Pazos, C. Formulation of
785 resveratrol entrapped niosomes for topical use. *Colloids Surf, B* **2015**,
786 *128*, 398–404.
- 787 (39) Devaraj, G. N.; Parakh, S. R.; Devraj, R.; Apte, S. S.; Rao, B. R.;
788 Rambhau, D. Release Studies on Niosomes Containing Fatty Alcohols
789 as Bilayer Stabilizers Instead of Cholesterol. *J. Colloid Interface Sci.* **2002**,
790 *251*, 360–365.
- 791 (40) Kremer, J. M. H.; Van der Esker, M. W.; Pathmamanoharan, C.;
792 Wiersema, P. H. Vesicles of variable diameter prepared by a modified
793 injection method. *Biochemistry* **1977**, *16*, 3932–3935.
- 794 (41) Pons, M.; Foradada, M.; Estelrich, J. Liposomes obtained by the
795 ethanol injection method. *Int. J. Pharm.* **1993**, *95*, 51–56.
- 796 (42) Justo, O. R.; Moraes, A. M. Kanamycin incorporation in lipid
797 vesicles prepared by ethanol injection designed for tuberculosis
798 treatment. *J. Pharm. Pharmacol.* **2005**, *57*, 23–30.
- 799 (43) Szoka, F. C., Jr. Preparation of liposome and lipid complex
800 compositions. U.S. Patent 5,549,910, 1996.
- 801 (44) Ghanbarzadeh, S.; Arami, S. Enhanced Transdermal Delivery of
802 Diclofenac sodium via conventional liposomes, ethosomes, and
803 transfersomes. *BioMed Res. Int.* **2013**, *2013*, 1–7.
- 804 (45) Antonietti, M.; Förster, S. Vesicles and liposomes: a self-assembly
805 principle beyond lipids. *Adv. Mater.* **2003**, *15*, 1323–1333.
- 806 (46) Wang, Z.; He, X. Dynamics of vesicle formation from lipid
807 droplets: Mechanism and controllability. *J. Chem. Phys.* **2009**, *130*,
808 094905.
- 809 (47) Lasic, D. D. The mechanism of vesicle formation. *Biochem. J.*
810 **1988**, *256*, 1–11.
- 811 (48) Janmey, P. A.; Kinnunen, P. K. J. Biophysical properties of lipids
812 and dynamic membranes. *Trends Cell Biol.* **2006**, *16*, 538–546.
- 813 (49) Silva, R.; Ferreira, H.; Little, C.; Cavaco-Paulo, A. Effect of
814 ultrasound parameters for unilamellar liposome preparation. *Ultrason.*
815 *Sonochem.* **2010**, *17*, 628–632.
- 816 (50) Yamaguchi, T.; Nomura, M.; Matsuka, T.; Koda, S. Effects of
817 frequency and power of ultrasound on the size reduction of liposome.
818 *Chem. Phys. Lipids* **2009**, *160*, 58–62.
- 819 (51) Lo, C. T.; Jahn, A.; Locascio, L. E.; Vreeland, W. N. Controlled
820 self-assembly of monodisperse niosomes by microfluidic hydrodynamic
821 focusing. *Langmuir* **2010**, *26*, 8559–8566.